NMR Behavior of the Aromatic Protons of Bovine Neurophysin-I and Its Peptide Complexes: Implications for Solution Structure and for Function†

Esther Breslow,*,‡ Vinod Sardana,‡,§ Ruba Deeb,‡ Elisar Barbar,∥,⊥ and David H. Peyton*,∥

Department of Biochemistry, Cornell University Medical College, New York, New York 10021, and Department of Chemistry, Portland State University, Portland, Oregon 97207-0751

Received August 12, 1994; Revised Manuscript Received November 23, 1994⊗

ABSTRACT: The NMR behavior of the aromatic protons of bovine neurophysin-I and its complexes was interpreted with reference to the 2.8 Å crystal structure of the dipeptide complex of bovine neurophysin-II and to mechanisms underlying the thermodynamic linkage between neurophysin dimerization and peptide binding. Large binding-induced shifts in the ring proton signals of Tyr-2 of ligand peptides (~0.5 ppm upfield and ~0.35 ppm downfield at 25 °C for the 3,5- and 2,6-ring protons, respectively) were demonstrated. Consistent with the crystal structure, and in disagreement with conclusions by other investigators, evidence is presented indicating the absence of dipolar contact between Tyr-2 ring protons and protein Phe ring protons. The large binding-induced shifts are attributed to a strong influence of proximal neurophysin carbonyl and disulfide groups on the bound Tyr-2 ring, of potential importance in binding specificity. Resolution of the behavior of neurophysin Phe residues -22 and -35 and of their proton NOE contacts provided insights into the conformational changes associated with peptide binding and with dimerization. Within the amino domain of the protein, as evidenced by the behavior of interface residue Phe-35 and its NOE contacts, binding-induced changes in the subunit interface appeared to involve principally the junction between this interface region and the 3,10-helix that connects it to the binding site in the liganded state. By contrast, as judged by the NOE contacts of His-80, the corresponding interface participant of the carboxyl domain, peptide binding induced a marked decrease in side-chain mobility within the carboxyl domain segment of the interface. Interactions of Phe-22 with protons assigned to Ala-68, neither of which is an interface participant, were demonstrated to be markedly altered both by dimerization in the unliganded state and by peptide binding to the dimer. Since Phe-22 is adjacent to the peptide-binding site, the results collectively support a model in which conformational differences between unliganded monomer and dimer are important contributors to the preferential binding of peptide to the dimer and indicate that the amino and carboxyl domain segments of the interface, which are homologous, are affected differently by peptide binding.

The crystal structure of the complex of bovine neurophysin-II (NP-II)[1] with the peptide *p*-iodo-Phe-TyrNH$_2$ has been solved at 2.8 Å (Chen et al., 1991). In this complex, as demonstrated by solution studies [reviewed in Breslow and Burman (1990)], the dipeptide serves as a surrogate for neurophysin's physiological ligands, oxytocin and vasopressin; preliminary crystallographic analysis of the oxytocin complex of bovine NP-II confirms a conformation virtually identical to that of the dipeptide complex (Rose et al., 1991). While the crystal structure of liganded neurophysin therefore is available, the unusual thermodynamics of peptide binding to neurophysin (Breslow & Burman, 1990) and the preferential binding of peptide to the neurophysin dimer (Nicolas et al., 1980) raise questions about the conformation of unliganded neurophysin, which has not been crystallized. Neurophysin is a relatively small protein (92−95 residues per chain), and NMR would seem to be a reasonable approach to the study of this conformation. However, the dimer is the principal species present under 2D NMR conditions; relatively broad resonance signals and the recently demonstrated presence of multiple conformations in the unliganded dimeric state (Breslow et al., 1992b) have hindered complete conformational analysis by NMR.

In an attempt to deal with some of the complexities of neurophysin NMR spectra, we have focused on an analysis of the aromatic proton region [e.g., Breslow et al (1992b)]. Bovine neurophysins contain a single tyrosine and three phenylalanine residues per chain, in addition to a single histidine only in bovine NP-I [e.g., Breslow and Burman (1990)]. Since one of the Phe residues (Phe-91) can be excised without any effect on function (Rabbani et al., 1982; Sardana & Breslow, 1984) and can be shown not to

† Supported by Grant GM-17528 from the NIH. A preliminary report of this work was presented at the Eighth Symposium of The Protein Society (Breslow et al., 1994).

* Authors to whom correspondence should be addressed.

‡ Cornell University Medical College.

§ Present address: Merck Research Laboratories, West Point, PA 19486.

∥ Portland State University.

⊥ Present address: Department of Biochemistry, University of Minnesota, St. Paul, MN 55108.

⊗ Abstract published in *Advance ACS Abstracts,* January 15, 1995.

[1] Abbreviations: NP, neurophysin; NMR, nuclear magnetic resonance; 1D, one-dimensional; 2D, two-dimensional; NOE, nuclear Overhauser effect; NOESY, 2D nuclear Overhauser and exchange spectroscopy; DQF-COSY, 2D double-quantum-filtered *J*-correlated spectroscopy; TOCSY, 2D total correlation *J* spectroscopy; ROESY, 2D rotating-frame nuclear Overhauser spectroscopy; Phe-PheNH$_2$, L-phenylalanyl-L-phenylalanine amide; ^{D}Phe-PheNH$_2$, perdeuterated L-phenylalanyl-L-phenylalanine amide; Phe-TyrNH$_2$, L-phenylalanyl-L-tyrosine amide; *p*-iodo-Phe-TyrNH$_2$, *p*-iodo-L-phenylalanyl-L-tyrosine amide; Tyr-PheNH$_2$, L-tyrosyl-L-phenylalanine amide; TSP, sodium 3-(trimethylsilyl)propionate-d_4.

0006-2960/95/0434-2137$09.00/0

contribute significantly to 2D ^{1}H NMR spectra (vide infra), and since the single tyrosine can be nitrated without an effect on function (Furth & Hope, 1970), the aromatic region spectrum can be somewhat simplified and partially dissected. In this paper, we explore the behavior of the aromatic protons of neurophysin and its peptide complexes with particular emphasis on two questions. First, how is the chemical shift of bound peptide aromatic protons related to the crystal structure of the neurophysin−peptide complex? Such information is essential to attempts to cross-correlate the NMR spectra of liganded and unliganded states with the crystal conformation. Recent NMR studies by others (Lippens et al., 1993) have in fact been interpreted to indicate contacts between bound hormone and protein that would violate predictions made from the crystal structure (see Results), an interpretation shown here to be incorrect. Second, how do the properties of the two central phenylalanyl residues (Phe-22 and Phe-35) respond to changes in the state of the protein? Phe-35 is a direct participant in inter-subunit interactions in the dimer and is distant from the binding site, while Phe-22 is adjacent to the peptide-binding site in the crystal structure and is distant from the subunit interface (Chen, 1991; Chen et al., 1991). The responses of these two residues to dimerization in the unliganded state and to peptide binding therefore have the potential to illuminate mechanisms involved in the preferential binding of peptide by the dimer and the associated ligand-induced increase in the dimerization constant (Nicolas et al., 1980; Breslow et al., 1991). A central question about this mechanism, for example, is the extent to which conformational factors underlying this effect represent intra-subunit conformational differences between monomer and dimer in the unliganded state as opposed to conformational changes induced by peptide binding (Breslow et al., 1991, 1992b).

As in other studies of this system [e.g., Breslow et al. (1992b)], the neurophysin chosen for NMR studies is bovine NP-I, which is more soluble than bovine NP-II at NMR concentrations, but which has not yet been crystallized. The two neurophysins are highly homologous, however [reviewed in Breslow and Burman (1990)], with only small differences between the two observed in a large number of studies [e.g., Nicolas et al., (1980); Breslow et al., 1991, 1992b]. The crystal structure of liganded bovine NP-II is used as a guide in identifying resonances and has permitted a number of internally consistent assignments.

MATERIALS AND METHODS

Proteins and Peptides. Bovine NP-I and its des-1−8 derivative were prepared as described earlier [e.g., Peyton et al. (1986); Breslow et al., 1992b]. Removal of residues 90−92 of bovine NP-I was accomplished by treatment with carboxypeptidase A (Rabbani et al., 1982; Sardana & Breslow, 1984). Nitration of native bovine NP-I and its des-1−8 derivative (yielding protein mononitrated at Tyr-49) was accomplished also as described elsewhere [e.g., Huang et al. (1993)].

Phe-TyrNH_2 and Phe-PheNH_2 were obtained from Bachem Bioscience Inc. Perdeuterated Phe-PheNH_2 was synthesized from perdeuterated L-phenylalanine as described earlier (Peyton et al., 1987). Tyr-PheNH_2 was a gift from Dr. John Rose. Oxytocin was obtained from Sigma.

NMR Studies. Samples were typically dissolved directly in D_2O in the absence of buffer and adjusted to the desired pH (uncorrected electrode reading) with NaOD or DCl. D_2O concentrations used were 99.99% and 99.9% for studies at 500 and 400 MHz, respectively. Signals from nonexchanged amide protons, when present, were identified by their loss of intensity with time. One-dimensional spectra at 500 MHz were obtained using the Rockefeller University 500 MHz spectrometer with an internal reference of TSP. Two-dimensional spectra (vide infra) were referenced to TSP through the HDO resonance at 4.76 ppm at 25 °C and at 4.56 ppm at 45 °C. All values are reported as ppm downfield from TSP.

Two-dimensional spectra were recorded at 400.14 MHz on a Bruker AMX-400 NMR spectrometer. The 2−3 mM samples were 0.4−0.5 mL in 5 mm NMR tubes at the temperatures and pH values indicated. The 90° observation pulse was 8−9 μs, and the relaxation delay was set to 2 s, during which a low-power pulse was applied to saturate the residual water resonance. Data sets were acquired as 1024 points in t_2 and 512 points in t_1 and then zero-filled to give 1024 × 1024 (real) spectra after Fourier transformation. Phase-shifted sine-bell-squared windows were used for resolution enhancement. The phase shift was 38° for NOESY spectra; values of 60−80° were used for ROESY spectra. Baseline straightening was performed with the Bruker UXNMR software package.

Typical pulse sequences were used for obtaining the NMR spectra. Thus, NOESY (Kumar et al., 1980), DQF-COSY, (Rance et al., 1983), TOCSY, (Braunchweiler & Ernst, 1983), and ROESY (Bothner-by et al., 1984; Bax & Davis, 1985) were recorded in the phase-sensitive mode by the time-proportional incrementation method (TPPI) (Marion & Wüthrich, 1983). The integrity of the sample was checked by recording and comparing the 1D NMR spectrum for each sample before and after the 2D run. For ROESY experiments, artifacts arising from Hartman−Hahn matching can be especially troubling. Such cross-peaks were tested for by varying the locking frequency by up to 1200 Hz and the locking power by as much as a factor of 3. All cross-peaks between resonances in the 6−8 ppm region were found to be in the reported phase consistently under all conditions. Specific conditions are reported in the caption for each figure.

Measured chemical shifts at 400 MHz are 0.03 ppm upfield from those at 500 MHz (cf., Breslow et al., 1992b). Data are uncorrected for these differences. The NMR data were correlated with the crystal structure using coordinates from the laboratory of Dr. B.-C. Wang, as summarized in Chen (1991) and Chen et al. (1991).

RESULTS

Chemical Shifts of Bound Peptide Protons. Peptides that bind to the hormone-binding site of neurophysin must contain a nonpolar aromatic residue in position 2—Tyr or Phe binding with essentially equivalent affinity, Trp much more weakly, and His or nonaromatic residues apparently not at all (Breslow et al., 1973). There is less specificity for the residue in position 1 of the bound peptide, although peptides with aromatic residues in this position typically bind more strongly than their aliphatic counterparts (Breslow et al., 1973; Breslow & Burman, 1990). We have determined the chemical shift of several of the aromatic protons of bound peptides, in part by nitrating the single neurophysin tyrosine (Tyr-49) in order to move the chemical shift of its ring

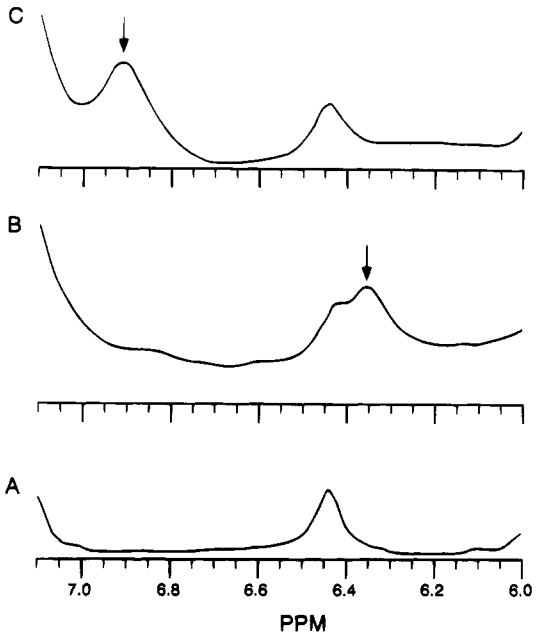

FIGURE 1: 500 MHz proton spectra of nitrated NP-I in D_2O in the presence of (A) saturating concentrations of ^{D}Phe-PheNH$_2$, (B) equimolar Phe-TyrNH$_2$, and (C) equimolar Phe-PheNH$_2$. Conditions: 3 mM protein; pH 6.0; 25 °C. Arrows in parts B and C point to signals assigned to bound protons from peptides Tyr-2 and Phe-2, respectively.

protons downfield from 7 ppm. It is relevant to these studies that, at 25 °C and pH 6, the interactions of these peptides with native or native nitrated neurophysin are typically associated with slow exchange kinetics on the NMR time scale relative to the chemical shift changes under consideration; exceptions are noted. First-order dissociation rate constants of 2−9 and 100 s^{-1} have been calculated for the complexes of oxytocin and Phe-TyrNH$_2$, respectively, under these conditions; second-order association rate constants are $\sim 10^6$ M^{-1} s^{-1} for both peptides (Pearlmutter & Dalton, 1980; Blumenstein et al., 1984).

Figure 1A shows the 6.0−7.2 ppm spectrum of 3 mM nitrated NP at pH 6 saturated with perdeuterated Phe-PheNH$_2$ (^{D}Phe-PheNH$_2$); the single proton resonance at 6.44 ppm has been assigned to an α-proton of the dimer state (Breslow et al., 1992b) and represents the sole contribution of the ligated protein to this region of the spectrum. Parts B and C of Figure 1 show the spectra obtained in the presence of equimolar Phe-TyrNH$_2$ and Phe-PheNH$_2$ (not perdeuterated), respectively, conditions representing ~90% saturation. Phe-TyrNH$_2$ leads to an increase in proton intensity immediately upfield from 6.44 ppm; the signal does not arise from free peptide, which has no resonances in this region (Table 1). An analogous signal is seen upon binding Phe-TyrNH$_2$ to the native protein (data not shown). Analysis of this effect as a function of the fraction bound indicates that ~2 protons from the peptide are involved and that the new peak is centered at 6.38 ppm. No such signal is seen upon binding dipeptides with Phe in position 2—non-perdeuterated Phe-PheNH$_2$ (Figure 1C) or Tyr-PheNH$_2$ (Table 1). However, a similar change is seen upon binding oxytocin to bovine NP-I [vide infra and also reported by Lippens et al. (1993)] and upon binding vasopressin to bovine NP-II (A. A. Bothner-by, P. K. Mishra, and E. Breslow, unpublished results). Since both hormones contain tyrosine in position 2, the data allow unambiguous assignment of the new proton signal to ring

Table 1: Observed Chemical Shifts of Peptide and Hormone Aromatic Protons in the Free State and Bound to Neurophysin-I at pH 6[a]

	free state (ppm)	bound state (ppm)	Δppm
Phe-TyrNH$_2$			
Tyr-2 ε-H	6.85	6.36	+0.49
Phe-PheNH$_2$			
Phe-2 ε-H	~7.3[b]	6.91[c]	ca. +0.39
oxytocin			
Tyr-2 δ-H (45 °C)	7.19	~7.42 (broad)	−0.23
Tyr-2 δ-H (30 °C)	7.18	7.52, 7.37?	−0.34, −0.19?
Tyr-2 δ-H (25 °C)	7.20	7.55	−0.35
Tyr-2 ε-H (45 °C)	6.86	6.32	+0.54
Tyr-2 ε-H (25−30 °C)	6.84	6.30	+0.54
Tyr-PheNH$_2$			
Phe-2 ε-H	~7.3[b]	6.90[c]	~+0.4
Tyr-1 ε-H	6.86	6.72	+0.14

[a] Assignments of dipeptide ε-protons in the bound state are from 1D spectral shifts; bound oxytocin protons were assigned from both the 1D spectra and ROESY analysis. Shifts are at 25 °C unless otherwise indicated. [b] As with many other Phe ring spin systems, signals from individual protons have not been assigned. These signals are located in the 7.2−7.4 ppm region in the dipeptides studied here. An average chemical shift of 7.30 ppm is therefore used for all Phe ring protons [e.g., Bundi and Wüthrich (1979)]. [c] The designation of these protons as ε-protons is assumed, on the basis of the similarity of their binding-induced change in chemical shift to that of Tyr-2 ε-protons.

protons from bound peptide Tyr-2;[2] in the case of the hormones, however, the resolved bound signal is located at 6.30 ppm at pH 6 (Table 1). Study of the NMR exchange behavior of the ring protons of Tyr-2 of oxytocin in the presence of neurophysin (see the following) further establishes the 6.30 ppm signal as originating from the tyrosine 3,5-ring protons (ε-protons), as first reported by Lippens et al. (1993).

The large upfield shift of the 3,5-ring protons of bound peptide Tyr-2 is not unique to tyrosine. Upon binding non-perdeuterated Phe-PheNH$_2$ (Figure 1C), a broad new signal is seen at ~6.91 ppm that does not represent free peptide (Table 1). This signal is also seen with Tyr-PheNH$_2$ (Table 1), but it is not seen in the presence of Phe-TyrNH$_2$ (Figure 1B) and is assigned to ring protons from the bound Phe ring of peptide residue 2. Since ring proton signals from this residue in the free state are located at an average position of 7.3 ppm (Table 1), this represents a binding-induced chemical shift change for Phe ring protons in peptide position 2 similar to that for Tyr ring protons in position 2. By contrast, the ring protons of an aromatic residue in peptide position 1 are shifted less by binding (Table 1). Bound Tyr-PheNH$_2$ shows the broad signal at 6.91 ppm from bound Phe-2 protons and a sharper signal at ~6.72 ppm, which is assigned to ring protons from the Tyr in position 1, since it is not present with bound Phe-PheNH$_2$. By assuming that these are ε-ring protons, this represents a shift of ~0.15 ppm from the free state, compared with the ~0.5 ppm shift for ε-ring protons in position 2.

Chemical shifts of peptide aromatic protons in free and bound states are summarized in Table 1. Distinction between the chemical shifts of bound ε- and δ-protons of Tyr-2 was accomplished by ROESY. Figure 2 shows ROESY studies at 30 and 45 °C of the native protein and excess oxytocin at pH 6.2; studies were also performed at 25 °C, but exchange

[2] This conclusion was first reported as a footnote in Breslow et al. (1992b).

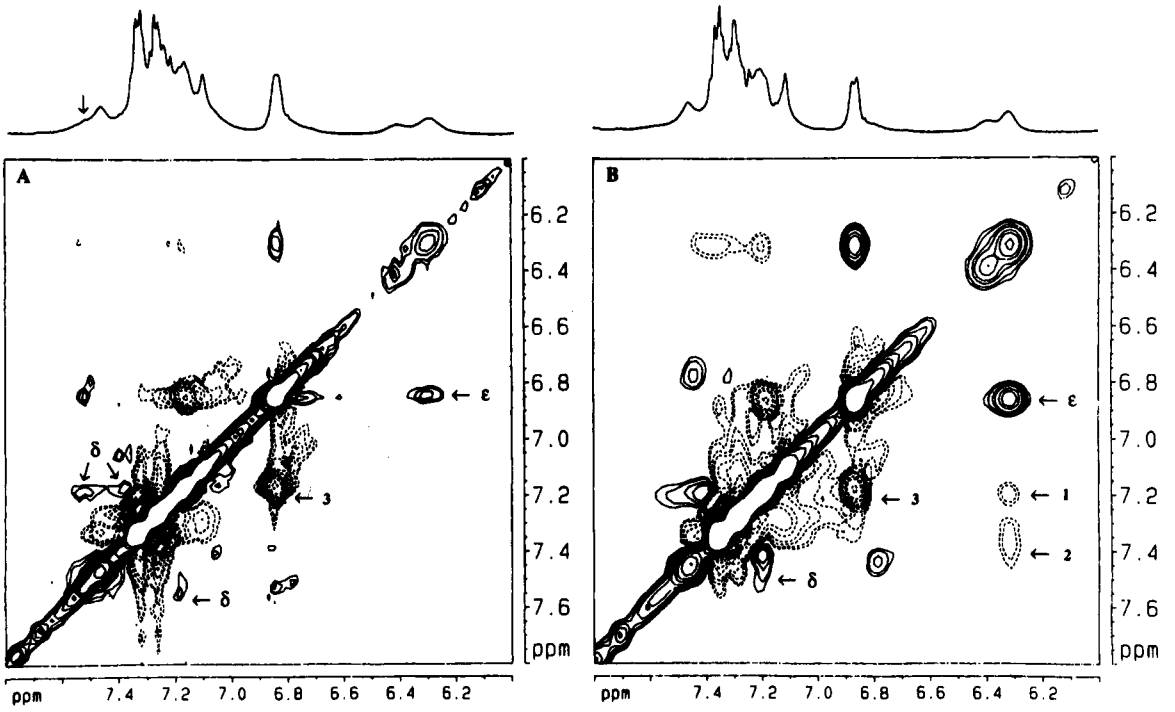

FIGURE 2: ROESY spectra of native NP-I in the presence of excess oxytocin at (A) 30 °C and (B) 45 °C. Conditions: ~3 mM protein; pH 6.2. These spectra were acquired at 400.14 MHz, with a spectral window of 4 kHz and 64 scans of 1024 points for each of the 512 t_1 increments. The mixing time was 50 ms, with a spin-locking power of 2 kHz. The residual H_2O resonance was suppressed by a low-power 1.5 s pulse. Solid off-diagonal lines: exchange cross-peaks; dotted lines: NOEs. Cross-peaks labeled ϵ and δ represent exchange between the bound and free states of ring protons of hormone Tyr-2; for reference, the chemical shifts of these protons in the free state are ~6.85 (ϵ-protons) and 7.2 ppm (δ-protons). Labeled NOE cross-peaks involving Tyr-2 are (1) bound ϵ-protons/unbound δ-protons, (2) bound ϵ-protons/bound δ-protons, and (3) composite cross-peak representing NOE between δ- and ϵ-ring protons of both the unbound Tyr-2 of oxytocin and the bound state of Tyr-49 from the protein. The composite nature of contributions to (3) accounts for its slight displacement relative to other signals from free Tyr-2 protons. The arrow in the 1D spectrum at 30 °C points to the signal from bound Tyr-2 δ-protons, which is seen to be shifted in the 45 °C spectrum; this shift is reversible.

between free and bound states for the hormone and native protein is slower under these conditions, and exchange cross-peaks are weak. At 45 °C, the spectrum shows three principal exchange cross-peaks (6.32/6.86, 7.2/~7.42, and 6.78/7.45 ppm). Of these, the last is similar to a cross-peak seen in the ROESY spectra of the protein saturated with ^{D}Phe-PheNH$_2$ (data not shown) and therefore is not currently assigned to oxytocin exchange; its origin remains uncertain.[3] The 6.32/6.86 ppm cross-peak represents exchange of the ϵ-protons of the oxytocin tyrosine between free (6.86 ppm) and bound states (6.32 ppm); this cross-peak is diminished in intensity but shifted only trivially at 30 °C. The 7.2/~7.42 ppm cross-peak seen at 45 °C is assigned principally to the exchange of the oxytocin tyrosine δ-protons between the free (7.2 ppm) and bound (7.42 ppm) states. Assignment of the bound protons to 7.42 ppm is approximate; this chemical shift represents what appears to be the center of mass of a broad band that is distorted by neighboring NOEs. This exchange cross-peak shows significant temperature sensitivity; while weaker at 30 °C, it remains discernible as a very broad signal, but with two possible components representative of the bound state centered at ~7.52 and 7.37 ppm, respectively. The temperature sensitivity of the bound δ-proton signal can also be seen in the 1D spectra (Figure 2) and from the NOE peaks between the bound ϵ-ring protons at 6.3 ppm and the chemical shifts representative of the bound δ-protons at the different temperatures (cf., Figures 2 and 4); potential explanations include a nonequivalence between the two bound δ-protons, with increased averaging at higher temperatures due to faster ring rotation (see Discussion), or different conformational substates. At 25 °C, the location of the principal component of the δ-proton exchange cross-peak is 7.2/7.55 ppm (free/bound) (e.g., Table 1 and Figure 4), the same location assigned at 22 °C and pH 2 by Lippens et al. (1993) to a transfer NOE between the δ-protons of the oxytocin tyrosine and the ring protons of Phe-22 of the protein; the 7.2/7.55 ppm ROESY exchange peak was also present at pH 2 (data not shown). It is relevant that a poorly resolved weak exchange cross-peak at ~7.2/7.48 ppm, arising solely from protein Phe resonances (see the following), can be seen in the ROESY spectra of the protein saturated with ^{D}Phe-PheNH$_2$ (Table 2), but this peak can be differentiated from the exchange peaks near this location in the oxytocin complex by its shape, intensity, and lack of shift with temperature (data not shown).

The exchange properties of the Tyr-2 ϵ- and δ-protons are seen particularly clearly with the oxytocin complex of

[3] Observation of the 6.78/7.42 ppm exchange cross-peak as a function of temperature indicates that neither of its two components tracks with signals from Tyr-2 ϵ-protons. Also, while the chemical shift of the downfield component is similar to that of bound δ-protons at several temperatures, no exchange with free δ-protons (7.2 ppm) is seen, and at 45 °C, the upfield component of this cross-peak corresponds to a region of the 1D spectrum of little proton intensity (e.g., Figure 2). Nonetheless, the exchange peak appears to increase in intensity with increasing oxytocin concentration. Therefore, we cannot exclude the possibility, for example, that the cross-peak represents exchange in the environment of bound δ-protons. It is also relevant that this exchange cross-peak is not seen in spectra of the nitrated des-1−8 protein in the presence of oxytocin (Figure 3), but can be seen in the corresponding spectra of the nitrated native protein (data not shown), indicating that it does not arise from Tyr-49.

Table 2: Intra-Phenylalanyl Connectivities of Signals from the Ring Protons of Phe-22 and Phe-35 in Unliganded and Liganded States at pH 6.2, 25 °C[a]

NOESY cross-peak	ROESY	COSY	TOCSY
	Unliganded State		
7.54/7.36	NOE	+	+
7.54/7.23	exchange[c]	absent	+
7.54/7.16	absent[e]	absent	*d*
7.54/7.06[b]	absent	*d*	+
7.36/7.16	exchange	*d*	+
7.36/7.06[b]	absent	*d*	*d*
7.33/7.25	NOE[d]	*d*	*d*
7.25/7.05	exchange	*d*	+
	Liganded State		
7.48/7.23	NOE	+	+
7.48/7.21	absent[f]	absent	+
7.32/7.21	NOE	*d*	+
7.30/7.10	NOE	*d*	*d*

[a] ROESY, COSY, and TOCSY data for the liganded state were obtained in the presence of ^{D}Phe-PheNH$_2$; this complex shows the same Phe proton NOESY cross-peaks as that of the oxytocin complex. Other footnotes indicate results at pH 3 or at higher temperature that significantly differ from the pH 6, 25 °C data. [b] Absent at pH 3. [c] Gives an NOE in ROESY spectra at pH 3. [d] Ambiguous. [e] Gives an exchange cross-peak in ROESY spectra at pH 3. [f] Manifest as an exchange cross-peak at 40 °C. Its absence at 25 °C is assumed to represent NOE/exchange cancellation.

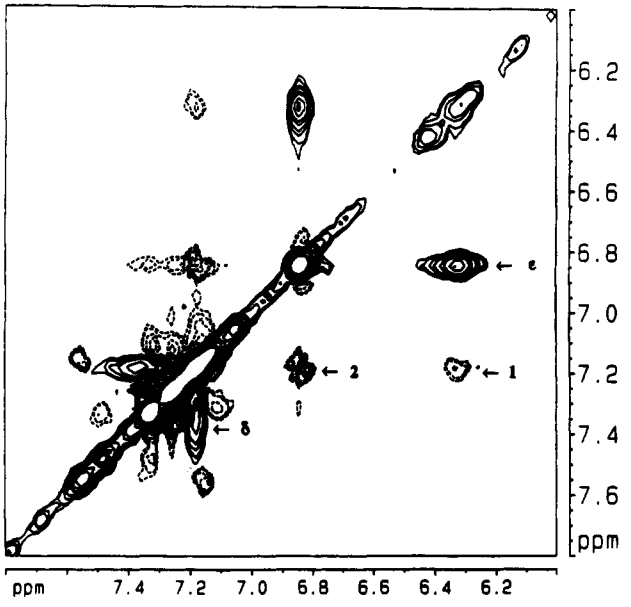

FIGURE 3: ROESY spectrum of nitrated des-1−8 NP-I in the presence of excess oxytocin. Conditions: ~2 mM protein; pH 6.2; 25 °C. This spectrum was acquired at 400.14 MHz, with a spectral window of 4 kHz and 96 scans of 1024 points for each of the 512 t_1 increments. The mixing time was 50 ms, with a spin-locking power of 2 kHz. The residual H_2O resonance was suppressed by a low-power 1.5 s pulse. Exchange cross-peaks for Tyr-2 ϵ- and δ-protons are labeled as in Figure 2. NOE cross-peaks are (1) bound Tyr-2 ϵ-protons/free Tyr-2 δ-protons and (2) free Tyr-2 ϵ-protons/free Tyr-2 δ-protons. Note the perfect alignment of exchange and NOE cross-peaks for Tyr-2 protons in the nitrated protein. NOE cross-peaks not seen in Figure 2 (e.g., 7.15/7.57 ppm) are from nitrotyrosine.

the nitrated des-1−8 protein (Figure 3). Nitration of Tyr-49 separates the NOE cross-peaks of the oxytocin tyrosine from those of the protein tyrosine, allowing improved visualization of the alignment of hormone exchange and NOE cross-peaks (see the legends to Figures 2 and 3). Moreover, the nitrated des-1−8 derivative binds more weakly than the native protein because it lacks Arg-8 (Sardana & Breslow, 1984), giving rise to very strong chemical exchange ROESY cross-peaks, even at 25 °C. The exchange cross-peaks of the tyrosine ϵ-ring protons in the nitrated des-1−8 protein (6.84/6.32 ppm) are essentially the same as those in the native and nitrated native proteins. The broad δ-proton exchange cross-peak (7.18/7.33 ppm) precisely aligns with the Tyr-2 δ- and ϵ-proton NOE cross-peaks, with the shape of the peak suggesting two possible components as in the complex of the native protein. However, in this case, the signal from the bound state appears to be centered ~0.2 ppm upfield from that in the complex of the native protein at the same temeprature, the results indicating a potential influence of Arg-8 and/or nitration of Tyr-49 on the chemical shift of bound Tyr-2 δ-protons.[4]

Behavior of the Ring Protons of Neurophysin Phe-22 and Phe-35. Neurophysin Phe ring protons exhibit exchange behavior, particularly in the unliganded state, that complicates their NMR assignments. The complexity reflects the NMR properties of Phe-22 and Phe-35. Phe-91 proton signals have been assigned earlier in 1D spectra as a series of sharp multiplets in the region 7.2−7.4 ppm (Sardana & Breslow, 1984). Comparison of NOESY spectra of the native protein with spectra of the functionally normal des-90−92 protein also indicates that, with the exception of some easily recognized artifacts in the vicinity of these sharp multiplets, Phe-91 makes little contribution, presumably because of its mobility; e.g., NOE cross-peaks between aromatic and nonaromatic protons are identical in the spectra of the native and the des-90−92 proteins under our conditions (data not shown). Accordingly, data from both the native and des-90−92 proteins were used to analyze the behavior of Phe-22 and Phe-35 protons.

Figure 4 shows the aromatic proton region NOESY spectra of ~2 mM des-90−92 NP at pH 6.3 alone and in the presence of excess oxytocin. The unliganded protein is ~80% dimer by weight under these conditions and the liganded protein in 100% dimer by weight (Nicolas et al., 1980), a fact relevant to the analysis of the data because Phe proton signals are altered by dimerization [e.g., Peyton et al. (1986); Breslow et al., 1992b]. The weight fraction of dimer can be calculated from the relative intensities in 1D spectra (not shown) of the signals at 6.4 and 6.2 ppm, representing the slowly exchanging dimer and monomer states, respectively, of the same α-proton (Breslow et al., 1992b); concomitantly, a strong monomer/dimer (exchange) cross-peak at 6.2/6.4 ppm for this α-proton is seen in the NOESY spectrum of the unliganded protein that is absent in the presence of oxytocin (Figure 4).

The 7.0−7.6 ppm region in Figure 4 contains the Phe ring proton signals plus the δ-proton signals of Tyr-49 (7.06 ppm in the unliganded state and 7.18 ppm in the liganded state [e.g., Peyton et al. (1987)] and of Tyr-2 of oxytocin when present (vide supra). The C-4 proton of His-80 is also present, but gives NOESY cross-peaks under the conditions here only in the liganded state (vide infra). NOESY cross-

[4] Attempts to distinguish between the effects of nitration and of cleavage of residues 1−8, by examination of oxytocin complexes of the nitrated native protein, were frustrated by very poorly resolved cross-peaks in this system. This resulted from overlap between signals from the nitrotyrosine and the hormone, together with weak chemical exchange cross-peaks.

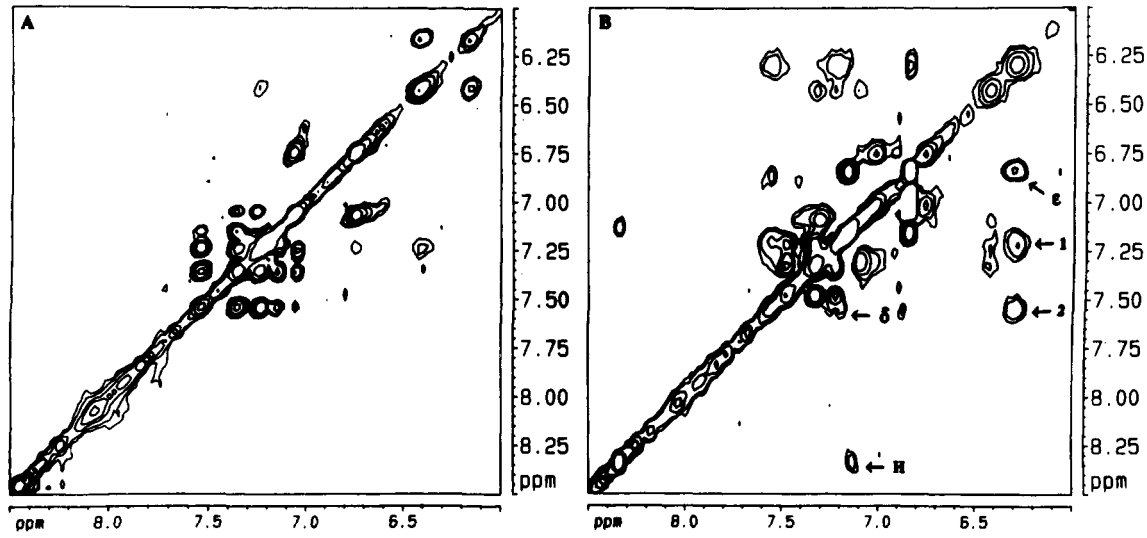

FIGURE 4: NOESY spectra of the aromatic proton region of des-90–92 NP-I in the absence (A) and presence (B) of oxytocin. Conditions: 2 mM protein; pH 6.3; 25 °C. These spectra were acquired at 400.14 MHz, with a spectral window of 4 kHz and 96 scans of 1024 points for each of the 512 t_1 increments. The mixing time was 100 ms. The residual H_2O resonance was suppressed by a low-power 1.5 s pulse. In (A), all cross-peaks that lie *completely* in the region 7.0–7.6 ppm are assigned to Phe. In (B), cross-peaks (or parts thereof) labeled δ and ϵ represent the exchange peaks between the free and bound states of hormone Tyr-2 protons. Note that the δ-proton exchange peak is seen as an extension of a Phe proton NOE peak. Other cross-peaks are identified as follows: (H) NOE between the C-2 and C-4 of His-80; (1) NOE between bound ϵ-protons and free δ-protons of oxytocin Tyr-2; and (2) NOE between bound ϵ-protons and bound δ-protons of oxytocin Tyr-2.

peaks assignable to Phe-22 and Phe-35 ring protons are listed in Table 2. These cross-peaks were examined further by ROESY, COSY, and TOCSY at pH 6, with the results also given in Table 2. Data for the unliganded protein were also obtained at pH 3, which differs from the unliganded state at pH 6 in that the dimerization constant is higher and the protein is effectively all dimer at these concentrations (Peyton et al., 1986); Table 2 indicates those NOESY peaks that are lost at pH 3. Data for the liganded protein were obtained both with oxytocin (Figure 4) and with ^{D}Phe-PheNH$_2$ (Table 2); the spectra indicate virtually identical Phe proton NOE connectivities in the two complexes. It is relevant to these data that the most downfield Phe proton signal, located at 7.54 ppm in the unliganded state and at 7.48 ppm in the liganded state, is unique to the dimer state and appears to represent a single Phe proton (Peyton et al., 1986; Breslow et al., 1992b). Therefore, its connectivities potentially describe just one of the two Phe spin systems.

Of the Table 2 cross-peaks that occur in the unliganded state at pH 6, the 7.54/7.36 ppm cross-peak is unremarkable, giving an NOE on ROESY and the COSY and TOCSY behavior expected for two adjacent ring protons; this behavior is unchanged at pH 3. The 7.36/7.16 ppm cross-peak behaves as clear exchange on ROESY at both pH 6 and 3, but it also gives a TOCSY, suggesting that these positions reflect the nonequivalent ϵ- or δ-protons of the same slowly rotating ring. However, the other cross-peaks of the unliganded state give more complex behavior. At pH 6, the 7.54/7.23 ppm cross-peak shows up as exchange in the ROESY spectrum and gives a TOCSY, but the ROESY behavior changes to an NOE at pH 3. The 7.54/7.16 ppm cross-peak is absent from ROESY spectra at pH 6, suggesting a cancellation of exchange and NOE effects, but is manifest as exchange at pH 3. The 7.54/7.06 and 7.36/7.06 ppm peaks are also absent from ROESY spectra at pH 6 and, significantly, are absent from NOESY spectra at pH 3. A 7.25/7.05 ppm peak was located in a region of the ROESY spectrum too crowded to be clearly identified. It is clear from the chemical shifts that there is too much overlap among the spin systems of Phe-22 and Phe-35 in the unliganded state to resolve completely the contributions of the two rings from these data alone.

The situation is much improved in the liganded state. Earlier spectra demonstrate that the 7.54 ppm Phe ring proton of the unliganded state moves upfield to ~7.48 ppm in the liganded state [e.g., Peyton et al. (1987)]. In the liganded state (Figure 4 and Table 2), the spin system associated with the 7.48 ppm signal gives three cross-peaks—at 7.48/7.32, 7.48/7.21, and 7.32/7.21 ppm. The 7.32/7.21 ppm peak behaves analogously to the 7.36/7.23 ppm peak of the unliganded state. The 7.48/7.32 ppm peak of the liganded state, like the 7.54/7.36 ppm peak of the unliganded state, shows the TOCSY and COSY connectivities expected for two adjacent protons. Similarly, the 7.48/7.21 ppm peak of the liganded state, like the 7.54/7.23 ppm peak of the unliganded state, shows evidence of both NOE and exchange components, as manifest in the former instance by NOE/exchange cancellation in the ROESY spectra. Separate from this spin system is a strong, well-resolved 7.30/7.10 ppm cross-peak. The separate identities of the two Phe ring spin systems in the liganded state are seen most clearly in their aliphatic connectivities (Figure 5). A large number of connectivities to a spin system with signals at 7.48, 7.32, and 7.21 ppm are seen, while a smaller number of aliphatic protons (e.g., 0.26 and 4.16 ppm) show discrete connectivities to a ring system with signals at 7.30 and 7.10 ppm.

One probable reason for the improved resolution of the two spin systems in the liganded state is the absence of monomer, as some of the complexities of the 2D maps of the unliganded state at pH 6 potentially reflect monomer–dimer exchange or the presence of multiple conformers of the unliganded dimer (Breslow et al., 1992b) that might exchange via dimer dissociation. This is supported by the fact that the 7.06 ppm signal associated with the 7.54 ppm spin system of the unliganded state appears to be lost both

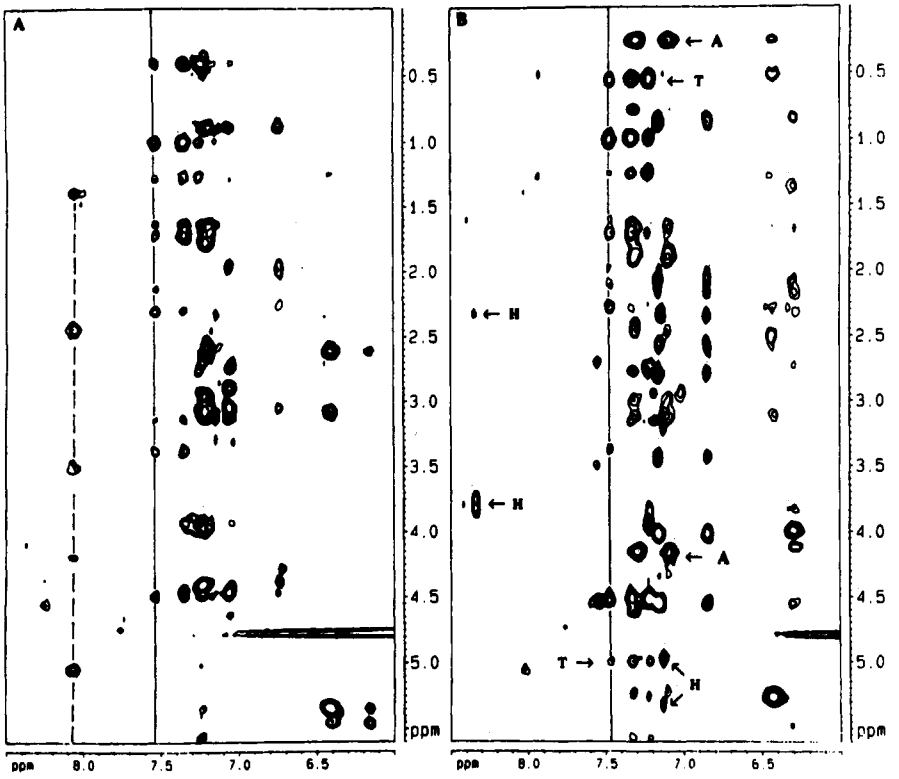

FIGURE 5: NOESY spectra showing aromatic/aliphatic region connectivities of des-90−92 in the absence (A) and presence (B) of oxytocin. Conditions are the same as in Figure 4. In (A), the dashed line indicates connectivities to nonexchanged amide protons at 8.08 ppm. The solid line represents aliphatic connectivities to the most downfield Phe signal (7.54 ppm), assigned to Phe-35. No connectivities to His ring protons (e.g., C-2 at ~8.45 ppm) are seen. In (B), the solid line represents aliphatic connectivities to the most downfield Phe signal (7.48 ppm), assigned to Phe-35 in the liganded state. Other cross-peaks are as follows: (A) Phe proton connectivities to Ala-68; (T) Phe proton connectivity to the γ- and α-protons of Thr-38 (Phe proton connectivities to the β-protons of Thr-38 are not marked, but can be seen at 4.54 ppm); (H) connectivities of the His-80 C-2 (8.3 ppm) and C-4 protons (7.13 ppm) to the aliphatic region.

at pH 3 and in the liganded state, with both conditions leading to an increase in the dimerization constant.

Assignment of Phe Ring Protons through Their Aliphatic Connectivities. The 7.54 ppm Phe ring proton of the unliganded state (7.48 ppm in the liganded state) had tentatively been assigned earlier to Phe-35 (Breslow et al., 1992). To verify this assignment and to locate Phe-22 proton signals, we assigned several aliphatic connectivities of the resolved Phe ring systems in the liganded state, using the crystal structure of the dipeptide complex as a guide.

The relevant connectivities that allowed the distinction between the two Phe ring systems are summarized in Table 3. In the liganded state, the 7.30 and 7.10 ppm signals were assigned to Phe-22 on the basis of their strong NOE connectivities to proton signals at 0.26 and 4.16 ppm (Figure 5). COSY and TOCSY studies (Table 3) identified the 0.26 and 4.16 ppm signals as the coupled β- and α-protons, respectively, of a discrete spin system, assignable to an Ala residue. A search of the environments of the rings of Phe-22 and Phe-35 in the crystal structure indicated only one Ala residue, Ala-68, with a methyl group close to a Phe ring. Two protons of this methyl group sit atop the ring face of Phe-22 with distances in the 3 Å range; the position of these protons relative to the ring is in reasonable accord with the upfield shift of this signal, when compared with an expected chemical shift of 1.39 ppm (Bundi & Wüthrich, 1979) for unperturbed peptide Ala methyl proton signals. Identification of the Phe-22/Ala-68 connectivity in the liganded state in turn facilitated identification of Ala-68 protons in the unliganded state. Earlier 1D studies had strongly suggested

Table 3: Assignment and Behavior of the Protons of Ala-68 and Thr-38

	liganded state connectivities (ppm)			
signal (ppm)	Phe proton NOE	COSY	TOCSY	assignment
	Phe-22			
0.26	7.1, 7.3	4.16	4.16	Ala-68, β-H
4.16	7.1, 7.3	0.26	0.26	Ala-68, α-H
	Phe-35			
0.53	7.48, 7.32, 7.21	4.54	4.54, 5.00	Thr-38, γ-H
4.54	7.48, 7.32, 7.21	0.53[a]	0.53[a]	Thr-38, β-H
5.00	7.48, 7.32, 7.21	*a*	0.53[a]	Thr-38, α-H
	unliganded state connectivities (ppm)			
signal (ppm)	Phe proton NOE	COSY	TOCSY	assignment
	Phe-22			
0.37	7.22[b]	3.95	3.95	Ala-68, β-H
3.95	7.32, 7.22	0.37	0.37	Ala-68, α-H
	Phe-35			
0.40	7.54, 7.36, 7.23	4.51	4.51, 5.0	Thr-38, γ-H
4.51	ambiguous	0.40, 5.00	0.40, 5.00	Thr-38, β-H
5.00	weak[c]	4.51	0.40, 4.51	Thr-38, α-H

[a] COSY and TOCSY connectivities between the 4.54 and 5.0 ppm signals were difficult to identify in the liganded state, but NOE connectivities between 4.54 and 5.0 ppm were very strong in this state. [b] Exact Phe connectivities are ambiguous because of overlap with the Thr-38 signal. [c] This connectivity is absent or weak depending on spectral processing. When present, it is manifest as very weak cross-peaks to 7.35 and 7.23 ppm; no connectivity to 7.54 ppm is seen.

that the 0.26 ppm peak of the bound state represents a binding-induced upfield shift of protons resonating near 0.4 ppm in the unliganded dimer (Peyton et al., 1987). The present studies of the unliganded state (Table 3, Figure 5)

demonstrate the presence of an Ala residue with β- and α-proton signals at 0.37 and 3.95 ppm, respectively, the latter showing NOE connectivity to Phe ring proton signals in the 7.2−7.3 ppm region, but none to 7.54 ppm, consistent with Phe-22 connectivity. The 0.37 ppm signal overlaps a signal assigned to Thr-38 in the unliganded state (vide infra), so that its Phe ring connectivity can be only partially isolated.

Assignment to Phe-35 of the spin system associated with the 7.54 ppm proton of the unliganded state and with the 7.48 ppm proton in the liganded state was independently supported by its connectivities to upfield protons assignable to Thr-38 (Table 3, Figure 5). In the liganded state, the 7.48 ppm spin system shows a strong NOE to protons at 0.53 ppm, which in turn show strong COSY and TOCSY connectivities to 4.54 ppm and weak TOCSY connectivity to 5.0 ppm. Strong NOE connectivity among the 0.53, 4.54, and 5.0 ppm signals was seen (data not shown), although 4.54/5.0 ppm *J*-coupling was difficult to demonstrate in the liganded state (Discussion). In the unliganded state, the 0.53 ppm signal shifts to 0.40 ppm, with maintenance of the strong NOE connectivities to 4.5 (4.51 ppm in this case) and 5.0 ppm and to the Phe ring spin system associated with the 7.54 ppm signal. This state shows strong TOCSY connectivities among the 0.53, 4.51, and 5.0 ppm signals and strong COSY 0.53/4.51 and 4.51/5.0 ppm connectivities. The data assign the spin system to a Thr residue, with γ-proton signals at 0.4 (unliganded state) and 0.53 ppm (liganded state), the β-proton signal at 4.5 ppm, and the α-proton signal at 5.0 ppm. Neurophysin-I has two Thr residues, −9 and −38. Inspection of the crystal structure (liganded state) indicates that Thr-38 should show the demonstrated NOE connectivities to Phe-35, while Thr-9 is distant from both Phe residues [e.g., Chen (1991); Chen et al., 1991]. In this structure, the γ-protons of each Thr-38 contact the ring of Phe-35 from both subunits, with the closest ring contacts (which are above the plane of the ring) to its partner subunit. Thus, these contacts should lead to upfield shifts of Thr γ-proton signals relative to their location at 1.2 ppm in unstructured peptides (Bundi & Wüthrich, 1979), in accord with what is seen, and to a strong chemical shift dimerization dependence, in accord with large spectral differences in this region between monomer and dimer (Peyton et al., 1986). Additionally, the crystal structure predicts weaker Phe ring NOE contacts to the β-protons of Thr-38 than to the γ-protons and very weak contacts to Thr α-protons, in agreement with the NOESY spectrum of the liganded protein (Figure 5).

Assignment of the chemical shifts of Phe-35 ring protons and of Thr-38 protons and resolution of the NOE connectivities to the Phe-35 ring provide a partial picture of binding-associated events at the region of the subunit interface containing these residues. Of particular interest is the comparison of aliphatic connectivities to the 7.54 ppm proton system in the unliganded state with those to the 7.48 ppm proton system in the liganded state, as seen in Figure 5. The overall pattern of connectivities is strikingly similar in both states, but there are some reproducible differences. Of these differences, the most readily identifiable arise from the change in chemical shift of Thr-38 γ-protons, to which the Phe ring protons show similar connectivities in both states, and the virtual loss of Phe ring proton connectivity to the Thr-38 α-proton signal at 5.0 ppm in the unliganded state. The other detectable differences in Phe-35 connectivities are the loss of a moderately intense 3.4/7.32 ppm cross-peak and of a very weak 3.15/7.54 cross-peak in the liganded state.

His-80 Ring Protons. His-80 is also located at the subunit interface (Breslow et al., 1992b), but in a segment separate from that containing Phe-35 (see Discussion). The ring protons of His-80 show very different behavior in liganded and unliganded states. As demonstrated earlier in 1D spectra, the C-2 proton signal is complex at pH 6.2 in the unliganded state and becomes a single peak when peptide is bound (Griffin et al., 1975). NOESY spectra here indicate the absence of both intra- and interresidue connectivities associated with the C-2 and C-4 ring protons of His-80 in the unliganded state at pH 6 (Figures 4 and 5). However, in the liganded state, at the same pH, the C-2 proton has a sharp signal at 8.45 ppm that shows strong NOE connectivity to the C-4 proton at 7.11 ppm. Additionally, the C-2 proton in the liganded state shows NOESY connectivity to aliphatic protons with signals at 3.75 and 2.3 ppm, while the C-4 proton shows a NOESY connectivity to 5.32 and 5.00 ppm (Figure 5 and related data). The data indicate that peptide binding is accompanied by a decrease in mobility or conformational substates of the His-80 ring that allows the development of strong intraring NOEs and also of NOEs from the ring to either the β- and α-protons of the same residue or to protons of other residues.[5]

Tyr-49 Ring Protons. The chemical shifts of Tyr-49 ring protons in liganded and unliganded states have been assigned previously (Balaram et al., 1973; Peyton et al., 1987; Breslow et al., 1992b). At pH 6, the shifts of the δ- and ϵ-ring protons shift from ~7.05 and 6.75 ppm, respectively, in the unliganded state to ~7.18 and 6.85 ppm, respectively, in the liganded state, the latter values depending somewhat on the identity of the bound peptide (Peyton et al., 1987). This change in chemical shift upon peptide binding is paralleled by other changes in tyrosine spectroscopic properties that in part suggest increased exposure of Tyr-49 to solvent on binding (Griffin et al., 1973). The crystal structure of the dipeptide complex also suggests that Tyr-49 is largely exposed to solvent in the liganded dimer; dimer−dimer contacts involving some Tyr-49 residues are seen in the crystalline dipeptide complex (Chen et al., 1991), but are probably of diminished importance in solution [e.g., Nicolas et al. (1980)]. Surprisingly, the data here indicate an increase in NOESY contacts to the Tyr-49 ring protons in the liganded state. This can be seen in Figure 5 by comparison of the cross-peaks to the ϵ-ring protons at 6.75 ppm in the unliganded state and at 6.85 ppm in the liganded state. Note that, with the exception of one at 2.2 ppm, all of the cross-peaks to 6.85 ppm in the liganded state seen in the oxytocin complex (Figure 5) can be demonstrated with complexes of perdeuterated Phe-PheNH_2, thereby precluding their identification as transfer NOE to the oxytocin tyrosine. The results suggest the possibility that, as with the surface residues of some other proteins, the exact orientation of Tyr-49 might be affected by crystal-packing forces.

DISCUSSION

The conclusion by Lippens et al. (1993) that the δ-protons of the Tyr-2 ring of bound oxytocin and the ring of

[5] Preliminary studies of 5 mM unliganded des-1−8 NP-I at pH 5.7 indicate His-80 NOE contacts similar to those reproducibly induced by peptide binding to native protein at pH 6.2. The results suggest the potential influence of a titratable group and/or of the 1−8 sequence on the carboxyl domain interface.

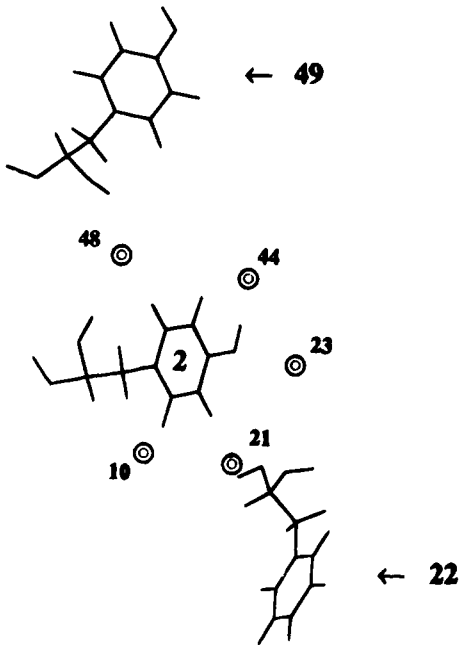

FIGURE 6: Relationship of bound peptide Tyr-2 to the rings of Tyr-49 and Phe-22 in the crystal structure of the dipeptide complex of bovine NP-II. Circles mark the positions of the S of Cys-10, the carbonyl oxygens of residues 21, 23, and 44, and the terminal oxygen of Asn-48. These atoms have closest approach distances to Tyr-2 ring carbons of 3.7, 3.6, 3.3, 3.3, and 3.1 Å, respectively. The carbonyl oxygen of Phe-22 approaches ring carbons of Tyr-2 at a closest distance of 3.8 Å. Specific distances to Tyr-2 ϵ-carbons are given in the text. The drawing is by Hyperchem using coordinates from the crystal structure of Chen et al. (1991).

neurophysin Phe-22 are in NOE contact in the complex is inconsistent with the crystal structure of the dipeptide complex of bovine neurophysin-II, as seen from Figure 6. In the crystal structure, the closest approach of these protons to Phe-22 ring protons is 6.7 Å, and no NOE should be observed. While the studies by Lippens et al. (1993) were conducted at pH 2.1, and while differences in the mode of binding of oxytocin and vasopressin at pH 2 and 6 have been demonstrated (Balaram et al., 1973; Live et al., 1987), our studies indicate no differences between pH 2 and 6 in the chemical shifts of bound Tyr-2 ring protons. Therefore, the demonstration of an NOE between the Tyr-2 δ-protons and the ring of Phe-22 would suggest that the structures of the complexes of oxytocin and of dipeptide differed, that the crystal structure was in error or did not apply in solution, or that there were unexpected differences between the binding sites of bovine neurophysin-I (the subject of the NMR studies) and bovine neurophysin-II (the subject of the X-ray structure). However, our results also indicate that Tyr-2 ϵ-ring protons in bound dipeptides show chemical shifts similar to those seen in bound oxytocin and that there is no difference between the two bovine neurophysins in this shift. Recent crystallographic data in fact indicate that Tyr-2 of oxytocin sits in the neurophysin binding pocket analogously to the dipeptide tyrosine (J. Rose and B.-C. Wang personal communication). Most directly, our results indicate that the conclusion concerning NOE proximity between the Tyr-2 δ-proton and a Phe ring proton probably represented a misinterpretation of the data. At 25 °C, at both pH 2 and 6, wer find a 7.2/7.5 ppm NOESY cross-peak that represents chemical exchange between the free and bound states of the δ-ring protons of Tyr-2; this cross-peak is analogous to that interpreted by these investigators to represent an NOE between the oxytocin Tyr-2 δ-protons (7.2 ppm) and a protein Phe ring proton (7.5 ppm). Finally, our data indicate that Phe protons with signals near 7.5 ppm in the liganded state arise from Phe-35, not Phe-22; Phe-35 is located at the subunit interface, distant from the peptide- and hormone-binding site (Chen, 1991).

Nonetheless, there are large binding-induced changes in the chemical shifts of hormone and peptide tyrosine ring protons, the origin of which should, in principle, be discernible from the crystal structure. Here we focus primarily on the binding-induced shifts in ϵ-proton resonances because these illustrate the complexity of the factors involved, and because these shifts can be compared with studies elsewhere (Blumenstein et al., 1980) of ^{13}C binding-induced shifts in oxytocin in which the ϵ-carbons of the Tyr-2 ring were ^{13}C-enriched. We observe an upfield shift of ~0.56 ppm in the average signal from both ϵ-protons upon binding that does not significantly change with temperature. Does this mean that both protons have the same environment in the bound state? Blumenstein et al. (1980) demonstrated that rotation of the Tyr-2 ring in the bound state is hindered, with estimated rotation rates of 130 and 900 s^{-1} at 20 and 42 °C, respectively. From these data, we estimate a rotation rate of ~230 s^{-1} at 25 °C. At 400 MHz, these rates limit the possible difference in chemical shifts between the two ϵ-ring protons to a maximum of ~0.15 ppm. The two ϵ-protons therefore might be nonequivalent in the bound state, but both are shifted upfield upon binding, with one proton necessarily shifting as much as 0.56−0.7 ppm. In attempting to account for this shift, one potential contribution is the hydrogen bonding of the phenolic hydroxyl, as seen in the crystal structure (Chen et al., 1991). However, given the similarity between peptide Phe-2 and Tyr-2 ring protons in binding-induced changes in chemical shift (Table 1), a contribution from hydrogen bonding of more than 0.1 ppm to the proton shift is unlikely. A second potential factor is a ring current effect from Phe-22 and/or Tyr-49. Although the ring protons of Phe-22 and of Tyr-2 are not in NOE contact, the crystal structure indicates that the two ϵ-ring protons of Tyr-2 approach the ring center of Phe-22 at distances of 7 and 10 Å, respectively. However, the orientation of the protons relative to the Phe ring is not optimal for maximum shielding in this case. Using the static geometry of the crystal, chemical shift calculations by the method of Johnson and Bovey (1958) predict no shielding of Tyr-2 ϵ-protons by the ring of either Phe-22 or Tyr-49, a calculation consistent with the observation that nitration of Tyr-49 does not affect the chemical shift of Tyr-2 ϵ-protons. Factors other than shielding by aromatic rings therefore must be involved, as also indicated in the following.

Insights into the complexity of the factors involved are provided by the ^{13}C shifts of the ϵ-carbons of Tyr-2 upon binding. Studies by Blumenstein et al. (1980) have shown that one ϵ-carbon is shifted upfield by 2.4 ppm, while the other is shifted downfield by 0.9 ppm, which is very different from the proton data and, when considered together with the proton data, very difficult to rationalize in terms of shielding/deshielding effects of neighboring aromatic rings. We suggest that a major factor affecting the binding-induced changes in the chemical shifts of Tyr-2 ϵ-atoms is the effect of proximal carbonyl and disulfides from the protein. In the crystal structure (e.g., see Figure 6), Tyr-2 ϵ-carbons

approach the amide oxygen of Asn-48 at a distance of 3.8 Å, the sulfur of Cys-10 at 3.7 Å, and four peptide bond carbonyl oxygens at distances of 3.3−3.9 Å. Preliminary CNDO calculations [e.g., Pople and Segal (1966), as calculated via Hyperchem] indicate that the binding pocket significantly alters the distribution of AMBER charges on ring carbon and hydrogen atoms (R. H. Haschemeyer and E. Breslow, unpublished results), an effect that would be expected to impact differently on ^{13}C shifts and proton shifts. (Note that hydrogen bonding of the phenolic OH might also be a contributor to the larger binding-induced changes in ^{13}C, but would not account for the fact that the two ϵ-ring carbons are shifted in different directions upon binding.) Further studies are needed to explore this suggestion. However, the recognition that the Tyr-2 ring is bound in an environment that is relatively rich in electronegative atoms might be useful in explaining the specificity of the binding pocket into which it inserts. No nonaromatic side chain has yet been found to insert into this pocket (Breslow & Burman, 1990), suggesting that the arrangement of dipoles in the pocket might be selective for ligand side chains of high polarizability.

By focusing on the aromatic residues of the protein, the present studies allow the first clear distinction between the aromatic proton resonances of Phe-22 and Phe-35 and, in turn, permit new insights into conformational change in this system. Of particular interest are the assignment of Phe-22 aromatic protons in the bound state and the consequent assignment of the most upfield proton signal in the bound state to the methyl protons of Ala-68. This signal, located at 0.26 ppm in the bound state (all dimer), is located at 0.38 ppm in the unbound dimer and is known from previous studies to be located no farther upfield than 0.64 ppm in the unliganded monomer, which has no signals upfield from this position [Peyton et al. (1986) and corresponding unpublished studies at 500 MHz]. Since the magnitude of the upfield shift of Ala-68 methyl protons is determined by the geometry of its relationship to the Phe-22 ring, the results indicate that this spatial relationship is significantly different in the unliganded monomer and unliganded dimer. Phe-22 borders the peptide-binding site (Figure 6), and both Phe-22 and Ala-68 are distant from the monomer−monomer interface (Chen et al., 1991). These results therefore confirm and extend conclusions from previous studies that the dimerization of unliganded NP-I is accompanied by a conformational change in the vicinity of the binding site. The first indication of such a change was a dimerization-induced change in the NMR signal from Tyr-49 (Peyton et al., 1986; Breslow et al., 1992b), which is located on the opposite side of the binding pocket from Phe-22 (Figure 6). This conformational change, which occurs without a demonstrable change in secondary structure (Breslow et al, 1992b), represents long-range communication between the subunit interface and the binding pocket and is of likely significance to allosteric mechanisms in this system.

Neurophysin was probably the first protein for which ligand-facilitated dimerization was demonstrated (Nicolas et al., 1976, 1980). The property of ligand-facilitated dimerization is now considered to play a fundamental role in the activity of many growth factor receptors (Vos et al., 1992), and we view neurophysin as an accessible paradigm with which to explore its basis. In neurophysin, the peptide-binding site and subunit interface are located on opposite sides of the molecule (Chen et al., 1991). Two mechanisms, not mutually exclusive, have been suggested as potential contributors to ligand-facilitated dimerization in the case of neurophysin—conformational differences between unliganded monomer and dimer that affect the binding site and changes in the subunit interface of the dimer associated with ligand binding (Breslow et al., 1991, 1992b). The effect of dimerization on the relationship between Phe-22 and Ala-68 clearly provides evidence in support of the former mechanism. However, the behavior of Phe-35 and His-80 resonances confirms change around and within the subunit interface upon ligand binding, as also suggested by studies of pressure-induced subunit dissociation (Breslow et al., 1991), and partially delineates these changes.

Neurophysin has two domains: a larger amino domain, in which the binding site and half of the subunit interface are located, and a smaller carboxyl domain, in which the other half of the interface is located. Interactions across the interface represent antiparallel β-sheets between like domains; the interface regions of the two domains are homologous (Chen, 1991; Chen et al., 1991). Phe-35 is located at the center of the amino domain interface region. With the exception of its contacts to Thr-38, Phe-35 is only modestly affected by peptide binding to the dimer, as evidenced by very limited changes in the chemical shift of its ring protons and in its other NOE contacts. These results are consistent with studies of this interface in ostrich neurophysin, in which Phe-35 is substituted by tyrosine; observation of the circular dichroism behavior of this tyrosine suggested little change upon peptide binding (Breslow et al., 1992a). On the other hand, the present data suggest changes in Thr-38. This residue is located at the end of the amino domain segment of the interface, representing a non-β-sheet residue that serves as a junction between the interface and the 3,10-helix that connects it to the binding site in the liganded state. Peptide binding is seen to alter the chemical shift of Thr-38 methyl protons, to reduce the efficiency of J-coupling of its α- and β-protons, and to increase the NOE connectivities between the Thr-38 α-proton and the ring protons of Phe-35. The results suggest that peptide binding induces only small changes within the amino domain segment of the interface, but alters the relationship of this segment to residues (39−49) that form the 3,10-helix of the liganded state. Significantly, Tyr-49, which is located at the other end of this helix, is also known to be profoundly affected by peptide binding [e.g., Breslow and Burman (1990)], suggesting significant conformational change across this region.

In contrast to the amino domain segment of the interface, the carboxyl domain interface appears to be internally altered by peptide binding, as evidenced by the behavior of His-80, which is located at the center of this segment of the interface (Chen, 1991). Under the conditions used here, the His-80 ring protons of the unliganded dimer show neither intra- nor interresidue NOE contacts, while such contacts are clearly evident in the liganded state (Figures 4 and 5). Earlier 1D studies had demonstrated a change in His-80 proton signals associated with ligand binding (Griffin et al., 1975). The present results indicate that this change involves a ligand-induced decrease in the mobility of the His-80 ring, or in the number of conformations that it samples, such that the buildup of a negative NOE is observed only in the liganded state. With the caveat that His-80 represents only about one-fifth of this segment of the interface, the results suggest that

the side chains of the carboxyl domain segment of the interface are more mobile in the unliganded state than those of the amino domain interface region and are pinned down only when the hormone-binding site is occupied. Such binding-induced interface changes within the carboxyl domain have the potential to account for the binding-induced decrease in the solvent penetrability of the interface (Breslow et al., 1991) and suggest that this domain, which does not contain any segment of the dipeptide-binding site, might principally serve to modulate dimerization.

In summary, studies of aromatic protons within neurophysin and its complexes point to (a) an important effect of the carbonyl and disulfide groups in the neurophysin-binding pocket on the properties of the bound tyrosine ring of oxytocin and related peptides and (b) a complex mechanism of ligand-facilitated dimerization that involves both a difference in tertiary structure between the unliganded monomer and unliganded dimer and binding-induced changes at the subunit interface. The latter are shown to involve alterations in the junction of the amino domain segment of the interface with the helix that connects it to the binding site and in the rigidity of the carboxyl domain segment of the interface. An attractive but untested hypothesis is that the changes at the helix−interface junction in the amino domain provide the path by which binding-induced changes are communicated to the carboxyl domain.

ACKNOWLEDGMENT

We are grateful to Dr. David Cowburn for access to the 500 MHz NMR facility at The Rockefeller University and to Francis Picart for his help with 500 MHz spectroscopy.

REFERENCES

Balaram, P., Bothner-by, A. A., & Breslow, E. (1973) *Biochemistry 12*, 4695−4704.
Bax, A., & Davis, D. G. (1985) *J. Magn. Reson. 65*, 355.
Blumenstein, M., Hruby, V. J., & Viswanatha, V. (1980) *Biochem. Biophys. Res. Commun. 94*, 431−437.
Blumenstein, M., Hruby, V., Viswanatha, V., & Chaturvedi, D. (1984) *Biochemistry 23*, 2153−2161.
Bothner-by, A. A., Stephens, R. L., Lee, J., Warren, C. D., & Jeanloz, R. W. (1984) *J. Am. Chem. Soc. 106*, 811−813.
Braunchweiler, L., & Ernst, R. R. (1983) *J. Magn. Reson. 53*, 521−528.
Breslow, E., & Burman, S. (1990) *Adv. Enzymol. Relat. Areas Mol. Biol. 63*, 1−67.
Breslow, E., Weis, J., & Menendez-Botet, C. J. (1973) *Biochemistry 12*, 4644−4653.
Breslow, E., LaBorde, T., Bamezai, S., & Scarlata, S. (1991) *Biochemistry 30*, 7990−8000.
Breslow, E., LaBorde, T., Saayman, H. S., Oelofsen, W., & Naude, R. J. (1992a) *Int. J. Pept. Protein Res. 39*, 388−396.
Breslow, E., Mishra, P. K., Huang, H.-b., & Bothner-by, A. A. (1992b) *Biochemistry 31*, 11397−11404.
Breslow, E., Deeb, R., Sardana, V., & Peyton, D. (1994) *Protein Sci. 3* (Suppl. 1), 133 (Abstract 463−S).
Bundi, A., & Wüthrich, K. (1979) *Biopolymers 18*, 285−297.
Chen, L. (1991) Ph.D. Thesis, University of Pittsburgh, Pittsburgh, PA.
Chen, L., Rose, J. P., Breslow, E., Yang, D., Chang, W.-R., Furey, W. F., Jr., Sax, M., & Wang, B.-C. (1991) *Proc. Natl. Acad. Sci. U.S.A. 88*, 4240−4244.
De Vos, A. M., Ultsch, M., & Kossiakoff, A. A. (1992) *Science 255*, 306−312.
Furth, A. J., & Hope, D. B. (1970) *Biochem. J. 116*, 545−553.
Griffin, J. H., Alazard, A. R., & Cohen, P. (1973) *J. Biol. Chem. 248*, 7975−7978.
Griffin, J. H., Cohen, J. S., Cohen, P., & Camier, M. (1975) *J. Pharm. Sci. 64*, 507−511.
Huang, H.-b., LaBorde, T., & Breslow, E. (1993) *Biochemistry 32*, 10743−10749.
Johnson, C. E., & Bovey, F. A. (1958) *J. Chem. Phys. 29*, 1012−1014.
Kumar, A., Ernst, R. R., & Wüthrich, K. (1980) *Biochem. Biophys. Res. Commun. 95*, 1−6.
Lippens, G., Hallenga, K., Van Belle, D., Wodak, S. J., Nirmala, N. R., Hill, P., Russel, K. C., Smith, D. D., & Hruby, V. J. (1993) *Biochemistry 32*, 9423−9434.
Live, D. H., Cowburn, D., & Breslow, E. (1987) *Biochemistry 26*, 6415−6422.
Marion, D., & Wüthrich, K. (1983) *Biochem. Biophys. Res. Commun. 113*, 967−974.
Nicolas, P., Camier, M., Dessen, P., & Cohen, P. (1976) *J. Biol. Chem. 251*, 3965−3971.
Nicolas, P., Batelier, G., Rholam, M., & Cohen, P. (1980) *Biochemistry 19*, 3565−3573.
Pearlmutter, A. F., & Dalton, E. J. (1980) *Biochemistry 19*, 3550−3556.
Peyton, D., Sardana, V., & Breslow, E. (1986) *Biochemistry 25*, 6579−6586.
Peyton, D., Sardana, V., & Breslow, E. (1987) *Biochemistry 26*, 1518−1525.
Pople, J. A., & Segal, G. A. (1966) *J. Chem. Phys. 44*, 3289−3296.
Rabbani, L. D., Pagnozzi, M., Chang, P., & Breslow, E. (1982) *Biochemistry 21*, 817−826.
Rance, M., Sorensen, O. W., Bodenhausen, G., Wagner, G., Ernst, R. R., & Wüthrich, K. (1983) *Biochem. Biophys. Res. Commun. 117*, 479−485.
Rose, J. P., Breslow, E., Huang, H.-b., & Wang, B.-C. (1991) *J. Mol. Biol. 221*, 43−45.
Sardana, V., & Breslow, E. (1984) *J. Biol. Chem. 259*, 3669−3679.

BI9418737